

Variation of Oxo-Transfer Reactivity of (Nitro)Cobalt Picket Fence Porphyrin with Oxygen-Donating Ligands

John Goodwin,^{*,†} Tigran Kurtikyan,[‡] Jean Standard,[§] Rosa Walsh,^{||} Bin Zheng,[†] Diedre Parmley,[†] James Howard,[†] Shaun Green,[†] Arthur Marduykov,[‡] and David E. Przybyla[§]

Department of Chemistry and Physics, Coastal Carolina University, P.O. Box 261954, Conway, South Carolina 29526-6054, Department of Chemistry, University of South Florida, Tampa, Florida, Department of Chemistry, Illinois State University, Normal, Illinois, and Molecular Structure Research Centre, National Academy of Science, Yerevan, Armenia

Received September 15, 2004

Derivatives of (nitro)cobalt picket fence porphyrin with oxygen-donating ligands have been prepared in solution and in the solid state. Crystal structures of two of these derivatives, $(\text{H}_2\text{O})\text{CoTpivPP}(\text{NO}_2)$ and $(\text{CH}_3\text{OH})\text{CoTpivPP}(\text{NO}_2)$, have been determined. The ethanol complex $(\text{C}_2\text{H}_5\text{OH})\text{Co}(\text{TPP})(\text{NO}_2)$ has been obtained and spectrally characterized using sublimed layers methodology. The formation constant and the ΔH° value of the association reaction with ethanol have been determined by FTIR measurements in CCl_4 solution. Catalytic oxygen activation and oxo-transfer reactions of these derivatives have been assessed in solution. Correlations between the oxo-transfer reactivity, thermodynamics, and characteristics of the nitro ligand show that although calculated and observed ONO vibrational spectra and bond lengths suggest activation of the NO_2 ligand and enhanced oxo-transfer reactions as seen in the analogous five-coordinate complexes, density functional theory calculations support that thermodynamics limits oxo-atom transfer reactions in these six-coordinate systems.

Introduction

Greatly enhanced reactivity of pentacoordinate (nitro)-cobalt porphyrins $\text{CoP}(\text{NO}_2)$ in oxo-transfer reactions utilizing molecular oxygen as the oxidant has been studied in dichloromethane solution.¹ These solution-phase systems were prepared by using hexacoordinate derivatives of cobalt tetraphenylporphyrin CoTPP and cobalt picket fence porphyrin CoTpivPP , in which a pyridine ligand was coordinated in the sixth coordination site. The original pyridine complex of $(\text{py})\text{CoTPP}(\text{NO}_2)$ was studied by Tovrog in the late 1970s and the phthalocyanine analogue later by Ercolani et al. for their potential use as dioxygen-activation/oxo-transfer catalysts,² but the five-coordinate species was not recognized as having enhanced oxo-transfer reactivity until much later. Similar oxidation reactivity of some six-coordinate and five-

coordinate (nitro)iron porphyrins was recognized in the mid-1990s by Castro³ and Scheidt.⁴ With nitrogenous bases, the five-coordinate species was generated¹ under two sets of conditions: (1) micromolar porphyrin concentrations in dichloromethane (DCM) solution using 3,5-dichloropyridine as the ligand and (2) millimolar porphyrin concentration in DCM solution but with the Lewis acid lithium ion added as the perchlorate salt (saturated in DCM). The five-coordinate species were observed with distinct visible and IR spectra due to the manipulation of the coordination equilibrium. In these systems, oxidation of alkenes was found to be possible without added cocatalysts, but the oxidation reactions were found to lack specificity. These catalytic reactions generated a wide range of oxygen-containing products including

* To whom correspondence should be addressed. E-mail: jgoodwin@coastal.edu.

[†] Coastal Carolina University.

[‡] National Academy of Science.

[§] Illinois State University.

^{||} University of South Florida.

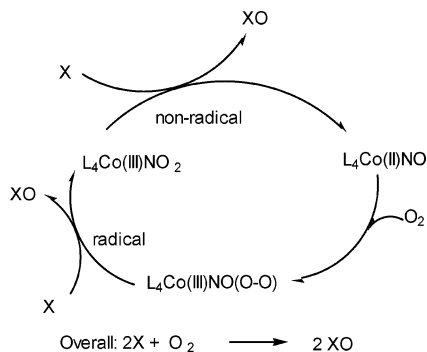
(1) Goodwin, J. A.; Bailey, R.; Pennington, W. T.; Rasberry, R.; Green, T.; Shasho, S.; Vongsavanh, M.; Echevarria, E.; Tiedeken, J.; Brown, C.; Fromm, G.; Lyerly, S.; Watson, N.; Long, A.; De Nitto, N. *Inorg. Chem.* **2001**, *40*, 4217–4225.

(2) (a) Tovrog, B. S.; Diamond, S. E.; Mares, F. *J. Am. Chem. Soc.* **1979**, *101*, 270–272. (b) Tovrog, B. S.; Mares, F.; Diamond, S. E. *J. Am. Chem. Soc.* **1980**, *102*, 6616–6618. (c) Tovrog, B. S.; Diamond, S. E.; Mares, F.; Stalkiewicz, A. *J. Am. Chem. Soc.* **1981**, *103*, 3522–3526. (d) Diamond, S. E.; Mares, F.; Szalkiewicz, A.; Muccigrosso, D. A.; Solar, J. P. *J. Am. Chem. Soc.* **1982**, *104*, 4266–4268. (e) Ercolani, C.; Paoletti, A. M.; Pennesi, G.; Rossi, G. *J. Chem. Soc., Dalton Trans.* **1991**, 1317–1321.

(3) O'Shea, S. K.; Wang, W.; Wade, R. S.; Castro, C. E. *J. Org. Chem.* **1996**, *61* (18), 6388–6395.

(4) Munro, O. Q.; Scheidt, W. R. *Inorg. Chem.* **1998**, *37*, 2308–2316.

epoxides, aldehydes, alcohols, and ketones, but the catalytic behavior persisted even in the presence of these potential oxygen-donating ligands at high concentration in solution. Minor spectral shifts were observed for the porphyrin catalysts during these reactions, but these were not explained in the initial studies. The proposed catalytic cycle provides for two distinct O-transfer steps.¹



The continued catalytic solution phase reactivity of the “five-coordinate” $CoP(NO_2)$ (where P = porphyrin) in the presence of oxygen-donating ligands suggested two possibilities: (1) that the hexacoordinate species formed from coordination also have enhanced catalytic activity or (2) that the kinetic lability and small stability constants of these oxygen-donating ligands with $CoP(NO_2)$ results in relatively high concentrations of the reactive five-coordinate complex.

The present work focuses on the structure and reactivity of hexacoordinate (nitro)cobalt picket fence porphyrins with oxygen-donating ligands including water and a selection of alcohols. Crystal structures of two new derivatives have been obtained, the formation of aqua, methanol, and ethanol complexes in solution has been studied spectroscopically, and the solution-phase stability and oxo-transfer reactivity of these complexes have been assessed. Further insight into the variation of oxo-transfer reactivity has been carried out with computational modeling using semiempirical PM3 and density functional theory (DFT).

Experimental Section

General Methods. Spectroscopic Methods. Routine infrared spectra were recorded using a Bomem Michelson FTIR system with an attenuated total reflection (ATR) attachment. Solution UV–visible spectra were recorded under nitrogen atmosphere using screw-capped 1-cm path length cells with a Hewlett-Packard 8453 diode array spectrometer or in a Vacuum-Atmospheres glovebox with an Ocean Optics PC1000 fiber optics spectrometer controlled by OOIBASE32 operating software. Evaluation of equilibrium constants from absorbance data was achieved using the SPECDEC program.⁵

Synthesis of Porphyrin Derivatives. The (nitro)cobalt(III) picket fence porphyrin, $LCoTpivPP(NO_2)$, derivatives were all prepared by the stoichiometric reaction of $Co(II)TpivPP$ (Midcentury Chemicals) with $AgNO_2$ (Acros Organics, 99%) in refluxing dichloromethane (Sigma) under nitrogen atmosphere in the glovebox

according to the method of Andrews.⁶ Unlike the previously studied $CoTPP$ derivatives, the $CoTpivPP(NO_2)$ preparation did *not* require the presence of an added nitrogenous base such as pyridine for the formation of the stable oxidized nitro complex and used the noncoordinating solvent DCM instead of CH_3CN . Silver nitrite is marginally soluble in DCM, but the suspension reacted with mild heating over several hours. The solid Ag byproduct was filtered from the solution before the solvent was removed under vacuum. Completion of the reaction was indicated by a single strong Soret band at 418 nm. The presence of coordinating impurities was detectable by broadening and red-shifts of this peak. All materials, except for dichloromethane solvent and alcohols used for synthesis, equilibrium, and reaction studies in these syntheses, were used as received. It was important to remove the amylene or cyclohexene stabilizer from this solvent prior to its use by washing with sulfuric acid, sodium hydroxide, and water before drying with calcium chloride and distilling from phosphorus pentoxide under nitrogen.⁷ Absolute ethanol and methanol were distilled from molecular sieves under nitrogen before transfer and use in the glovebox.

Crystals of (Aqua)(nitro)cobalt(III) Picket Fence Porphyrin, $(H_2O)Co(III)TpivPP(NO_2)$. Serendipitous growth of this crystalline product took place in a $CDCl_3$ solution used for an NMR sample, exposed to air.

Crystals of (Methanol)(nitro)cobalt(III) Picket Fence Porphyrin, $(CH_3OH)Co(III)TpivPP(NO_2)$. Growth of this crystalline product took place in attempts to isolate the pentacoordinate derivative, $Co(III)TpivPP(NO_2)$, under nitrogen atmosphere in the glovebox using the vapor diffusion method with a CH_2Cl_2 solution and hexane. Methanol contamination presumably arose from the glovebox atmosphere, since this solvent was present but was not intentionally added.

X-ray Crystallography. Data were collected using a Rigaku AFC8/Mercury CCD using graphite monochromated $Mo\ K\alpha$ radiation ($\lambda = 0.71073\ \text{\AA}$) at room temperature of $22 \pm 1\ ^\circ C$. The structures were solved by Direct Methods and refined using full-matrix least-squares on F^2 (SHELXTL PLUS).

Computational Modeling. Semiempirical PM3 and density functional theory (B3LYP 6-31G*) calculations were carried out using PC Spartan Pro or Spartan '04 (Wavefunction, Inc.) using cobalt porphine analogues in some cases to reduce computational time. Equilibrium geometries, heats of formation, and vibrational frequencies of the nitro ligands were determined for all of the six-coordinate $(L)CoP(NO_2)$ derivatives, where $L = H_2O, ROH$. No corrections were made to the calculated vibrational frequencies.

Reaction Studies. $(CH_3OH)CoTpivPP(NO_2)$ and other alcohol complexes were generated under nitrogen atmosphere by dissolving solid $(H_2O)CoTpivPP(NO_2)$ in methanol or other alcohols and evaporating the solution. The alcohol complexes could be prepared directly in solution by addition of alcohols to $CoTpivPP(NO_2)$ in dichloromethane. Visible spectra were recorded in glass cuvettes with a 1-cm path length. Simple oxo-transfer reactions of the nitro complexes with oxygen acceptors were carried out under nitrogen atmosphere to avoid reoxidation of any $CoTpivPP(NO)$ product with O_2 . Oxidation catalysis reactions were carried out under ~ 1 atm O_2 in vessels capped with oxygen-filled balloons. Organic product analysis was obtained by use of GC–MS analysis with a Hewlett-Packard model 6890 GC–MS instrument.

Infrared and UV–Vis Spectroscopy of Sublimed Layers. The five-coordinate nitro complex of $Co(TPP)$ has been obtained by

(5) Atkins, C. E.; Park, S. E.; Blaszek, J. A.; McMillin, D. R. *Inorg. Chem.* **1984**, *23*, 569–572.

(6) Andrews, M. A.; Chang, C.-T. T.; Cheng, C.-W. *Organometallics* **1985**, *4*, 268–274.

(7) Armarego, W. L. F.; Perrin, D. D. *Purification of Laboratory Chemicals*, 4th ed.; Butterworth-Heinemann: Boston, 1996.

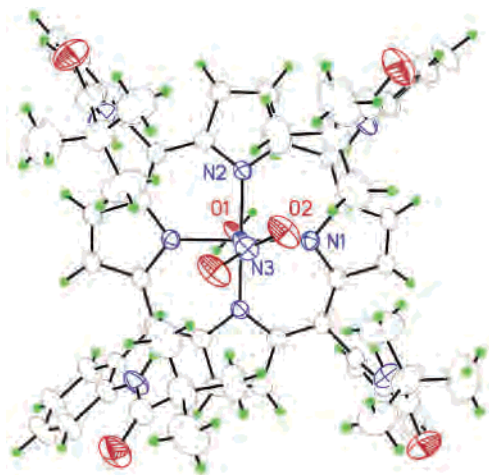


Figure 1. ORTEP diagram of $(\text{H}_2\text{O})\text{CoTpivPP}(\text{NO}_2)$.

interaction of NO_2 gas with a sublimed layer of $\text{Co}(\text{TPP})$ according to the procedure described earlier.⁸ Then the layer of $\text{Co}(\text{TPP})\text{-(NO}_2\text{)}$ was exposed to an atmosphere of alcohol vapor, the pressure of which was monitored by the mercury manometer connected with the optical cryostat. The layer was maintained at these conditions overnight, and then the excess of gaseous and adsorbed alcohols was eliminated by prolonged pumping out by the high vacuum system. The IR and UV-vis spectra of layers in vacuo have been measured by Specord M-80, Nicolet Nexus, and Specord M-40 spectrometers correspondingly. KBr (IR) and CaF_2 (UV-vis) were used as materials for optical windows and substrates.

Quantitative Measurements on $(\text{C}_2\text{H}_5\text{OH})\text{CoTPP}(\text{NO}_2)$ in CCl_4 Solutions. For the measurements of the ethanol complex, $(\text{C}_2\text{H}_5\text{OH})\text{CoTPP}(\text{NO}_2)$ obtained in thin films was quantitatively dissolved in CCl_4 and various quantities of rigorously dried ethanol were added to this solution. FTIR measurements have been done in the 0.06 cm width thermostated cell provided with KBr windows.

Results and Discussion

Crystal Structures. Figure 1 illustrates the ORTEP diagram of $(\text{H}_2\text{O})\text{CoTpivPP}(\text{NO}_2)$. Table 1 lists its crystal data and structure refinement, and Table S1 in the Supporting Information lists the crystallographic bond lengths and angles. Figure 2 illustrates the ORTEP diagram of $(\text{CH}_3\text{OH})\text{CoTpivPP}(\text{NO}_2)$. Table 2 lists its crystal data and structure refinement, and Table S2 in the Supporting Information lists the crystallographic bond lengths and angles. Two structures previously reported by Ohba et al. for $(\text{H}_2\text{O})\text{CoTPP}(\text{NO}_2)$ as the CH_2Cl_2 solvate⁹ and the dimethylformamide, DMF, disolvate¹⁰ demonstrate orientational disorder in the nitro and aqua ligand that results in an averaged structure in which the cobalt center has an inversion center. As in other (nitro) derivatives of iron¹¹ and cobalt picket fence porphyrins,¹² the solid state crystal structures presented here have the nitro ligand exclusively in the sterically hindered “pocket”, with no evidence of geometrical

Table 1. Crystal Data and Structure Refinement for $(\text{H}_2\text{O})\text{CoTpivPP}(\text{NO}_2)$

empirical formula	$\text{C}_{68}\text{H}_{70}\text{Cl}_{12}\text{Co N}_9\text{O}_7$	
formula weight	1609.66	
temperature	293(2) K	
wavelength	0.71073 Å	
crystal system	rhombohedral	
space group	$R\bar{3}c$	
unit cell dimensions	$a = 29.9186(10)$ Å $b = 29.9186(10)$ Å $c = 44.562(3)$ Å	$\alpha = 90^\circ$ $\beta = 90^\circ$ $\gamma = 120^\circ$
volume	$34544(3)$ Å ³	
Z	18	
density (calculated)	1.393 Mg/m ³	
absorption coefficient	0.697 mm ⁻¹	
$F(000)$	14904	
crystal size	$0.40 \times 0.40 \times 0.20$ mm ³	
θ range for data collection	1.82–24.76°	
index ranges	$-35 \leq h \leq 24$, $-33 \leq k \leq 35$, $-52 \leq l \leq 49$	
reflections collected	57315	
independent reflections	6582 [$R(\text{int}) = 0.0680$]	
completeness to $\theta = 24.76^\circ$	99.6%	
absorption correction	none	
max and min transmission	1.000 and 0.826	
refinement method	full-matrix least-squares on F^2	
data/restraints/parameters	6582/0/459	
goodness-of-fit on F^2	1.071	
final R indices [$I > 2\sigma(I)$]	$R1 = 0.0848$, $wR2 = 0.2509$	
R indices (all data)	$R1 = 0.1086$, $wR2 = 0.2727$	
largest diff peak and hole	1.322 and $-0.799 \text{ e} \cdot \text{Å}^{-3}$	

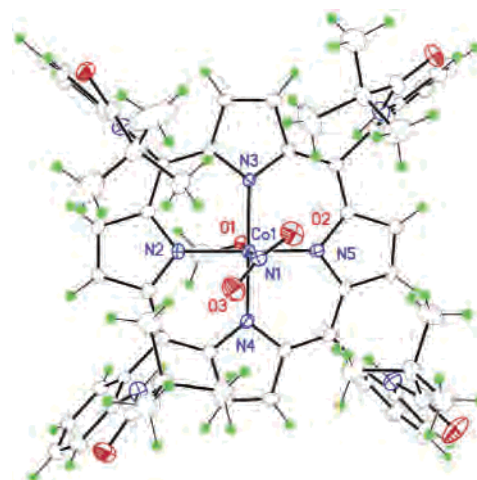


Figure 2. ORTEP diagram of $(\text{CH}_3\text{OH})\text{CoTpivPP}(\text{NO}_2)$.

isomers. The crystal structure of $(\text{EtOH})\text{CoTPP}(\text{NO}_2)$ ¹³ in contrast showed distinct coordination sites for the nitro ligand and the ethanol ligand. The method of crystal growth employed in that work combined ethanol and benzene solvents that depended on long-term stability of the complex in contact with ethanol at high concentration.

(8) (a) Kurtikyan, T. S.; Stepanyan, T. G.; Gasparyan, A. V. *Russ. J. Coord. Chem.* **1997**, *23*, 563–567. (b) Kurtikyan, T. S.; Stepanyan, T. G.; Gasparyan, A. V.; Zhamkochyan, G. H. *Russ. Chem. Bull.* **1998**, *47*, 695–698.

(9) Ohba, S.; Seki, H. *Acta Crystallogr.* **2002**, *E58*, m162–164.

(10) Ohba, S.; Eishima, M.; Seki, H. *Acta Crystallogr.* **2000**, *C56*, e555–e556.

(11) (a) Nasri, H.; Ellison, M. K.; Shang, M.; Schulz, C. E.; Scheidt, W. R. *Inorg. Chem.* **2004**, *43* (9), 2932–2942. (b) Nasri, H.; Ellison, M. K.; Krebs, C.; Huynh, B. H.; Scheidt, W. R. *J. Am. Chem. Soc.* **2000**, *122* (44), 10795–10804. (c) Ellison, M. K.; Schulz, C. E.; Scheidt, W. R. *Inorg. Chem.* **1999**, *38* (1), 100–108. (d) The product nitrate ligand observed from the reaction of coordinated nitrite in: Munro, O. Q.; Scheidt, W. R. *Inorg. Chem.* **1998**, *37* (9), 2308–2316. (e) Nasri, H.; Ellison, M. K.; Chen, S.; Huynh, B. H.; Scheidt, W. R. *J. Am. Chem. Soc.* **1997**, *119* (27), 6274–6283. (f) Nasri, H.; Haller, K. J.; Wang, Y.; Huynh, B. H.; Scheidt, W. R. *Inorg. Chem.* **1992**, *31* (16), 3459–3467. (g) Nasri, H.; Goodwin, J. A.; Scheidt, W. R. *Inorg. Chem.* **1990**, *29* (2), 185–191.

(12) Jene, P. G.; Ibers, J. A. *Inorg. Chem.* **2000**, *39*, 3823–3827.

(13) Ohba, S.; Seki, H. *Acta Crystallogr.* **2002**, *E58*, m183–m185.

Table 2. Crystal Data and Structure Refinement for (CH₃OH)CoTpivPP(NO₂)

empirical formula	C ₇₁ H ₇₉ CoN ₉ O ₇	
formula weight	1229.36	
temperature	100(2) K	
wavelength	0.71073 Å	
crystal system	monoclinic	
space group	P2(1)/n	
unit cell dimensions	$a = 14.9540(12)$ Å $b = 19.3065(14)$ Å $c = 22.0388(18)$ Å	$\alpha = 90^\circ$ $\beta = 92.809(2)^\circ$ $\gamma = 90^\circ$
volume	6355.2(9) Å ³	
Z	4	
density (calculated)	1.285 Mg/m ³	
absorption coefficient	0.332 mm ⁻¹	
F(000)	2604	
crystal size	0.10 × 0.10 × 0.02 mm ³	
θ range for data collection	1.40–28.30°	
index ranges	$-19 \leq h \leq 18$, $-9 \leq k \leq 22$, $-9 \leq l \leq 28$	
reflections collected	16170	
independent reflections	12716 [$R(\text{int}) = 0.0598$]	
completeness to $\theta = 28.30^\circ$	80.4%	
absorption correction	none	
refinement method	full-matrix least-squares on F^2	
data/restraints/parameters	12716/0/816	
goodness-of-fit on F^2	0.894	
final R indices [$I > 2\sigma(I)$]	$R1 = 0.0717$, $wR2 = 0.1444$	
R indices (all data)	$R1 = 0.1471$, $wR2 = 0.1734$	
largest diff peak and hole	0.868 and -0.391 e ⁻ Å ⁻³	

Crystal growth of the pentacoordinate derivative of (nitro)-cobalt picket fence porphyrin, CoTpivPP(NO₂), has eluded us, but a structure of pentacoordinate (nitro)cobalt tetraphenylporphyrin, CoTPP(NO₂), has also been reported by Ohba et al.¹⁴ as the benzene solvate. Its nitro ligand ONO bond angle was found to be 123.3(4)°,¹⁵ consistent with the relatively large angle predicted earlier by semiempirical methods.¹

Spectroscopy and Computational Modeling. Table 3 lists calculated equilibrium, bond angles, and vibrational frequencies for the nitro ligand determined by semiempirical calculations and the corresponding experimental results. No corrections were made for calculated vibrational frequencies. The corresponding measured IR values for the (ROH)-CoTPP(NO₂) analogues are also listed in Table 3B. Equilibrium geometries determined by semiempirical calculations showed good agreement with results from density functional theory for representative structures.

The layers of *meso*-tetraarylporphyrin metallo-complexes obtained by sublimation onto a low-temperature surface have a microporous structure¹⁶ similar to that of their bulk samples. Potential reagents can easily diffuse through the layer's bulk, and adducts thus formed can be spectrally characterized without masking effects of the solvent. Using this technique, the interaction of NO₂ gas with sublimed layers of CoTPP

Table 3. (A) Measured and Calculated Infrared Frequencies and ONO Bond Angles of (Nitro)cobalt Porphyrin Derivatives. (B) Infrared and Visible Spectral Characteristics for CoTPP(NO₂) Complexes with Alcohols Obtained in Sublimed Thin Films^a

Part A							
ligand	NO ₂ sym, cm ⁻¹		NO ₂ asym, cm ⁻¹		ONO angle		
	measd	PM3	measd	PM3	PM3	measd	PM3
none (five-coordinate)	1283	1674	1468	1853	none	NA	124.41
EtOH	1298	1689	1463	1841	1827	NA	122.67
<i>i</i> -PrOH	1301	1690	1462	1840	1825	NA	122.52
MeOH	1313	1688	1463	1845	1824	120.9	122.84
H ₂ O	1309	1693	1445	1842	1827	122.6	122.45
piperidine	1308	1701	1437	1837	1821	115.4	120.9
NH ₃	1309	1700	1431	1835	1817	NA	121.12
Cl ₂ py	1307	1701	1425	1835	1811	119.7	120.7
Py	1309	1702	1425	1835	1810	120.6	120.4
Me ₂ Npy	1310	1702	1427	1835	1810	NA	120.5
Im	NA	1701	NA	1835	1813	119.8	120.9
2MeIm	NA	1704	NA	1834	1811	120.4	120

Part B				
	$\nu_{\text{as}}(\text{NO}_2)$	$\nu_{\text{s}}(\text{NO}_2)$	$\delta(\text{NO}_2)$	λ (nm)
CoTPP·NO ₂	1468 (~1440)	1282 (1264)	805 (796)	533
R·CoTPP·NO ₂	1463 (1433)	1301 (1282)	809 (803)	541
R'·CoTPP·NO ₂	1463 (1431)	1298 (1278)	804 (798)	544
R''·CoTPP·NO ₂	1462 (1428)	1301 (1281)	804 (798)	545

^a R = CH₃OH, R' = C₂H₅OH, R'' = *i*-C₃H₇OH. In parentheses the data for the ¹⁵NO₂ isotopomer are given.

has been investigated previously and it has been shown that this process can be interrupted at the stage of five-coordinated nitro-complex formation.

It was predicted by Byrn and Strouse that five-coordinate axial complexes of metal-*meso*-tetraarylporphyrins conserve the microporosity of their structure and can serve as a template for designing of the metalloporphyrin axial complexes with the mixed ligands. This prediction has been confirmed by the study in which a number of six-coordinate nitro amino complexes of CoTPP were obtained by interaction of gaseous amines with the layers of CoTPP·NO₂.¹⁷ The same procedure has been used in this work with three alcohols, methanol, ethanol, and 2-propanol, and thereby, the formation of the six-coordinate nitro complexes of these species has been spectrally confirmed.

Figure 3 demonstrates the changes in the FTIR spectra of the CoTPP·NO₂ sublimed layer (solid line) after exposure in the atmosphere of ethanol (dashed line). This process resulted in shifting of the stretching modes of the coordinated nitro-group from their initial values. The $\nu_{\text{as}}(\text{NO}_2)$ CoTPP·NO₂ at 1468 cm⁻¹ undergoes a low-frequency shift and appears at 1463 cm⁻¹, while $\nu_{\text{s}}(\text{NO}_2)$ undergoes a high-frequency shift from 1283 to 1298 cm⁻¹. The same characteristic band-shifting is observed for 2-propanol with small deviations in frequencies listed in Table 3B. The fact that these bands and the deformational mode of the nitro-group $\delta(\text{NO}_2)$ undergo expected isotopic shifts in the experiments with ¹⁵NO₂ confirms the validity of this assignment. (Figure 4 and Table 3B). Additionally new bands denoted by asterisks appear in the spectra in the regions where the intense bands of alcohols are disposed. It is the bands at 3554 and

(14) Ohba, S.; Seki, H. *Acta Crystallogr.* **2002**, *E58*, m169–m171.

(15) Ohba, S., Department of Chemistry, Keio University, Hiyoshi 4-1-1, Kohoku-ku, Yokohama 223-8521, Japan, personal communication, July, 2004.

(16) (a) Kurtikyan, T. S.; Gasparyan, A. V.; Martirosyan, G. G.; Zhamkochyan, G. H. *J. Appl. Spectrosc.* **1995**, *62*, 62–66 (Russ.). (b) Byrn, M. P.; Curtis, C. J.; Hsiou, Y.; Khan, S. I.; Sawin, P. A.; Tendick, S. K.; Terzis, A.; Strouse, C. E. *J. Am. Chem. Soc.* **1993**, *115*, 9480–9497. (c) Byrn, M. P.; Strouse, C. E. *J. Am. Chem. Soc.* **1991**, *113*, 2501.

(17) Stepanyan, T. G.; Akopyan, M. E.; Kurtikyan, T. S. *Russ. J. Coord. Chem.* **2000**, *26*, 453–457.

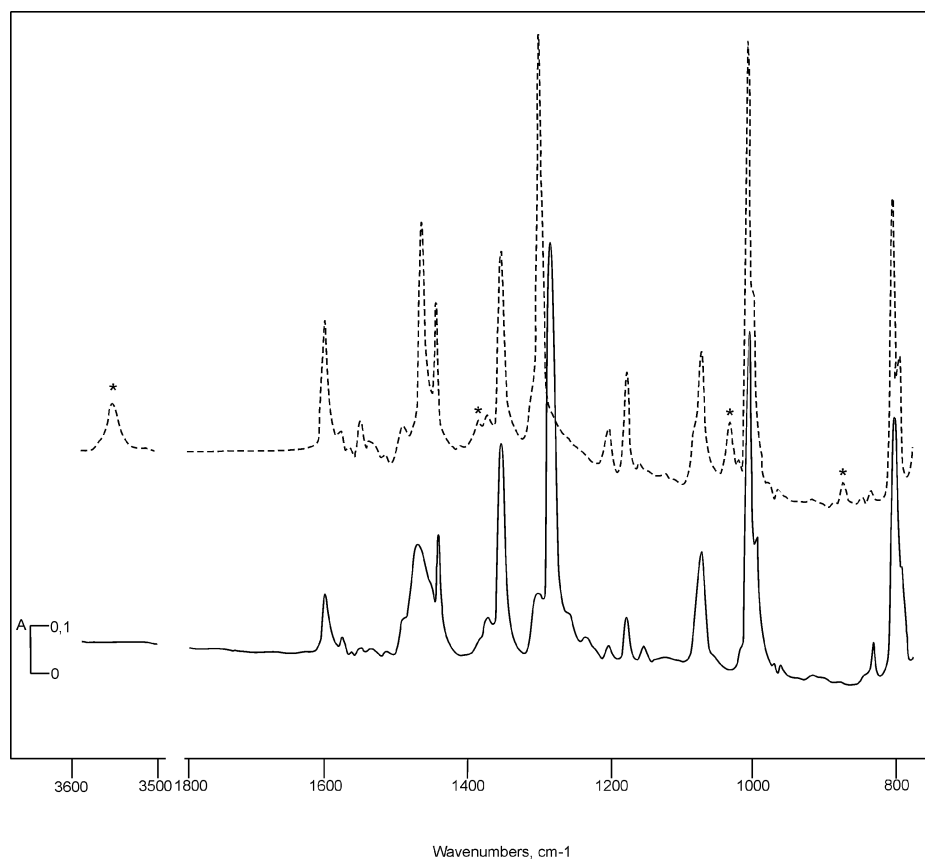


Figure 3. IR spectra of a sublimed layer of Co(TPP) after short time exposure under low pressures (10^{-1} mmHg) NO_2 (solid line) and additional exposure in an atmosphere of $\text{C}_2\text{H}_5\text{OH}$ (10 mmHg) overnight (dashed line).

1034 cm^{-1} that certainly belong to $\nu(\text{OH})$ and $(\text{C}-\text{O})$ of coordinated alcohol. Our gas-phase measurements show that for monomeric alcohols these bands are disposed in the range of 3660 and 1054 cm^{-1} correspondingly. Hence the coordination of alcohol through the oxygen leads to decreasing of $\nu(\text{OH})$ and $\nu(\text{C}-\text{O})$.

The results obtained in these thin-film experiments can be interpreted as evidence of formation of six-coordinate nitro alcohol complexes of Co(TPP). The UV-visible spectra give additional evidence for this conclusion. The band at 533 nm of $\text{Co}(\text{TPP})(\text{NO}_2)$ shifts to higher wavelengths in Table 3B and gains in intensity after interaction with alcohol in Figure 5. This behavior is also observed in solution where the visible spectra are quite similar as shown in Figure 6C. The directions of shifts in UV-visible and IR spectra upon additional coordination of alcohols are similar to those obtained in six-coordinate nitro complexes with amines. However, the magnitudes of shifts are larger for the latter that correlated with basicities of the sixth ligands. Notably this behavior qualitatively coincides with those predicted by calculations (Table 3A).

Lesser shifts of vibrational frequencies of the coordinated nitro-group in $\text{Co}(\text{TPP})(\text{NO}_2)$ upon additional coordination of alcohols compared with amines suggest that the electronic structure of the nitro-group in $(\text{ROH})\text{Co}(\text{TPP})(\text{NO}_2)$ is closer to those in five-coordinate complexes. This fact also suggests that six-coordinated nitro-alcohol complexes can also be active in oxo-transfer reactions performed by nitro complexes of Co(TPP).

Reactions. The unchanging visible spectrum of crystals of $(\text{H}_2\text{O})\text{CoTpvPP}(\text{NO}_2)$ dissolved in DCM under nitrogen atmosphere is shown in Figure 7. Addition of allyl bromide to this solution showed no change in the spectrum. Figure 6A shows the initial spectrum of $(\text{CH}_3\text{OH})\text{CoTpvPP}(\text{NO}_2)$ prepared by dissolving $(\text{H}_2\text{O})\text{CoTpvPP}(\text{NO}_2)$ in methanol after 2 min. Apparent in this figure is a shoulder at about 412 nm that grows over time to give the spectrum in Figure 6B. This resulting spectrum is identical to that previously observed for CoTpvPP in DCM with the Soret position at 412 nm , and its formation is attributable to methanolysis of the nitro ligand to NO. Similar behavior was observed in thin-film IR studies of the methanol complexes over time, with formation of $\text{CoTPP}(\text{NO})$ evident. The oxidized organic products of this reaction have not been isolated since the reaction was not catalytic and capable of producing large quantities of products even under oxygen-rich conditions, so it is not clear whether the oxidation of methanol itself is occurring in this system or what the reactive porphyrin species is.

In contrast, when the ethanol complexes were formed in the same fashion, the solutions retained the visible spectra represented in Figure 6C indefinitely, indicating no reaction of the (nitro)cobalt porphyrin ethanol complex with solvent ethanol. Addition of allyl bromide or cyclohexene to these ethanol solutions under nitrogen atmosphere also did not result in detectable change in the visible spectra. In contrast, addition of triphenylphosphine to the ethanol solutions under nitrogen resulted in a spectral shift of the porphyrin complex

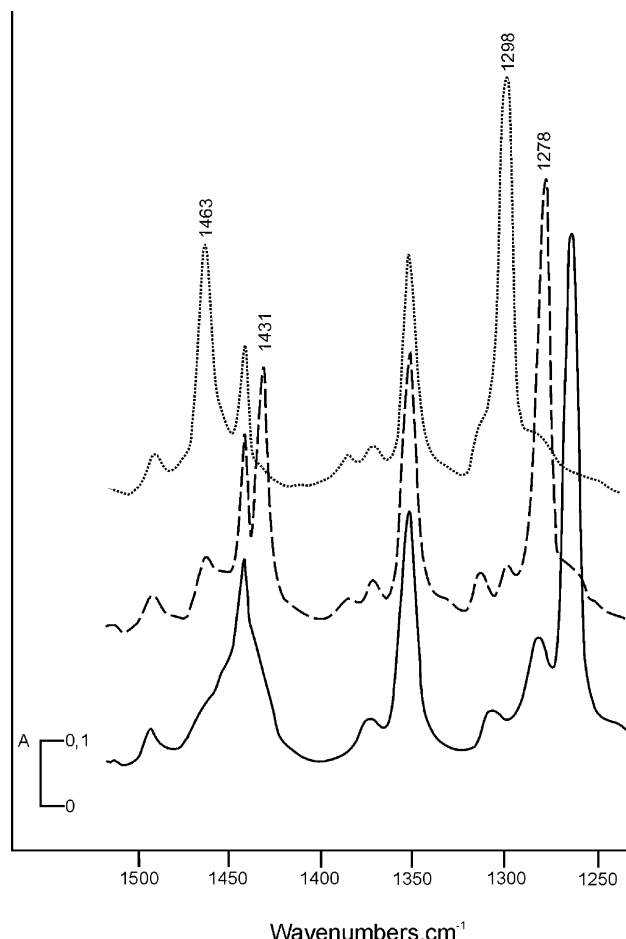


Figure 4. IR spectra of a sublimed layer of $\text{Co(TPP)}(^{15}\text{NO}_2)$ (solid line), $(\text{C}_2\text{H}_5\text{OH})\text{Co(TPP)}(^{15}\text{NO}_2)$ (dashed line), and $(\text{C}_2\text{H}_5\text{OH})\text{Co(TPP)}(\text{NO}_2)$ (dotted line).

Soret band from 429 to 412 nm, consistent with reduction of the porphyrin to $\text{CoTpvPP}(\text{NO})$. Carrying out this reaction under 1 atm O_2 in ethanol solutions resulted in nearly quantitative catalytic production of triphenylphosphine oxide confirmed by IR analysis and GC-MS.

Equilibrium measurements for the association of pyridine derivatives with $\text{CoTPP}(\text{NO}_2)$ were evaluated previously in DCM solution. The simplicity of the TPP system provided clear experimental results with isobestic behavior that were used to calculate stability constants of 7.0×10^6 and 1.1×10^8 for 3,5-dichloropyridine and pyridine, respectively.¹ Preparation of $\text{CoTpvPP}(\text{NO}_2)$ and $(\text{EtOH})\text{CoTpvPP}(\text{NO}_2)$ by the methods used in this work did not provide a series of visible spectra with clear isobestic points as the concentration of EtOH increased. This suggests that in the preparation of $\text{CoTpvPP}(\text{NO}_2)$ without the addition of pyridine or other bulky ligand, some fraction of product has the nitrite ligand in the tetrapivalamido pocket as expected, but due to the lack of selective coordination by the bulky pyridine on the exposed face, some fraction of the product has nitrite coordinated on the exposed face instead of within the pocket. While the crystal structures show only pocket-bound nitrite, it is likely that the crystalline packing favors this isomer in the crystallization or that separate crystals are indeed formed. Using the visible absorbance data collected with this

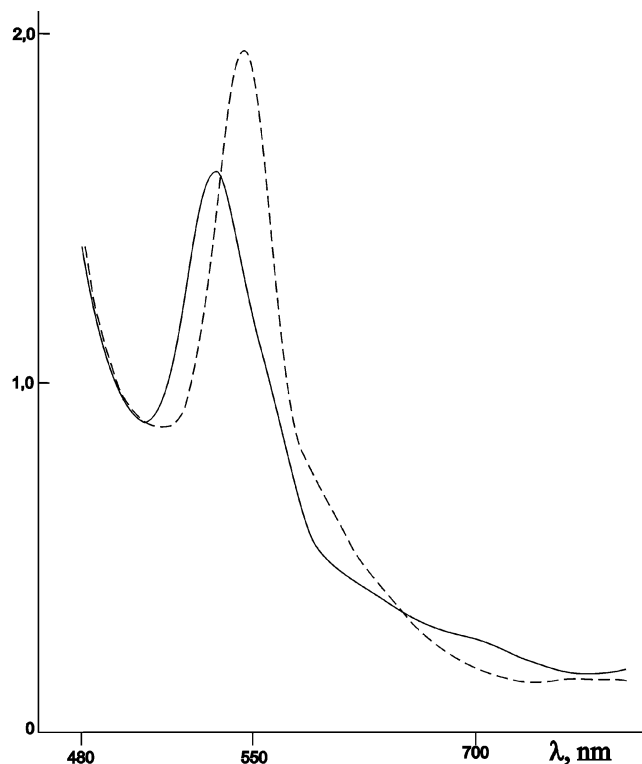


Figure 5. UV-visible spectra of a $\text{Co(TPP)}(\text{NO}_2)$ sublimed layer (solid line) after exposure under an atmosphere of ethanol (5 mmHg) within 2 h (dashed line).

proposed mixture of geometrical isomers, we were only able to obtain an estimate of the average stability constant for association of ethanol with $\text{CoTpvPP}(\text{NO}_2)$ with the SP-ECDEC program optimizing the results for a single ethanol coordination reaction. This value is approximately 350 in DCM. With stability constants this small, very large concentrations of an alcohol or other oxygen-donating ligand would be required to prevent significant formation of the reactive five-coordinate species. The lack of reactivity of ethanol solutions of $\text{CoTpvPP}(\text{NO}_2)$ with alkenes suggests that the six-coordinate alcohol complex predominates under these conditions and that this derivative is unreactive. A simplified system was used to better assess the equilibrium binding of ethanol spectroscopically in solution. Carbon tetrachloride solutions of $(\text{C}_2\text{H}_5\text{OH})\text{CoTPP}(\text{NO}_2)$ with various quantities of added ethanol are almost free from the IR bands of solvent and alcohol in the 1320–1270 cm^{-1} spectral region, in which the $\nu_s(\text{NO}_2)$ of coordinated nitro groups in five- and six-coordinate species are disposed. This allows measurement of concentration and temperature dependences of FTIR spectra to estimate the equilibrium constant K and ΔH° value of the association reaction. The symmetrical CoTPP derivative, of course, eliminates the problems encountered with the picket fence derivative described previously.

Figure 8 demonstrates the spectral changes observed upon addition of ethanol to a CCl_4 solution of $(\text{C}_2\text{H}_5\text{OH})\text{CoTPP}(\text{NO}_2)$. A well-defined isobestic point at 1293 cm^{-1} is seen as evidence of the presence of two species, $\text{CoTPP}(\text{NO}_2)$ and $(\text{C}_2\text{H}_5\text{OH})\text{CoTPP}(\text{NO}_2)$ with maximums of IR bands at 1283 and 1300 cm^{-1} , respectively.

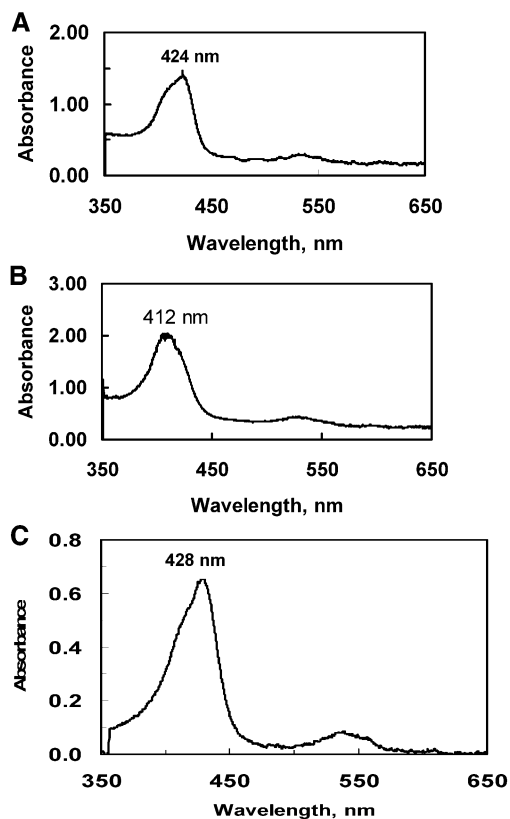


Figure 6. (A) Visible spectrum of unstable $(\text{CH}_3\text{OH})\text{CoTpivPP}(\text{NO}_2)$ prepared under nitrogen atmosphere from $(\text{H}_2\text{O})\text{CoTpivPP}(\text{NO}_2)$ crystals. The spectrum obtained 2 min after preparation shows initial decomposition with a shoulder at 412 nm. (B) Visible spectrum resulting from decomposition of $(\text{CH}_3\text{OH})\text{CoTpivPP}(\text{NO}_2)$ in methanol solution A. The formation of the peak at 412 nm is consistent with reduction to $\text{CoTpivPP}(\text{NO})$ by reaction with the solvent. (C) Stable visible spectrum of $(\text{CH}_3\text{CH}_2\text{OH})\text{CoTpivPP}(\text{NO}_2)$ in 3.5 M ethanol in CH_2Cl_2 , under nitrogen atmosphere.

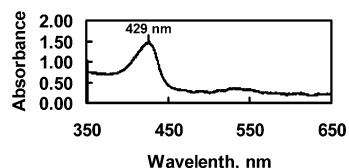
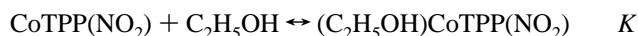


Figure 7. Visible spectrum of stable $(\text{H}_2\text{O})\text{CoTpivPP}(\text{NO}_2)$ in DCM solution prepared under nitrogen from $(\text{H}_2\text{O})\text{CoTpivPP}(\text{NO}_2)$ crystals.

The equilibrium constant of the reaction



at 25 °C derived from these spectra was found as $K = 9.8$. The ΔH° value of the association reaction calculated from the temperature dependence (Figure S1 in the Supporting Information) of equilibrium constants was -28 kJ/mol. The low value of this equilibrium constant indicates that in solution there is a significant quantity of five-coordinate species even at significantly higher molar equivalents of alcohol with respect to porphyrin nitro complex.

Computational modeling of the energies of formation of the six-coordinate products was pursued by use of DFT calculations, and the results are shown as standard enthalpies of formation at 298.15 K for the porphine or picket fence porphyrin models. No correction was made for solvation effects in the thermodynamics calculations. Standard heats

of formation of $\text{CoP}(\text{NO}_2)$, L, and $\text{LCoP}(\text{NO}_2)$ obtained in hartrees and converted to kJ/mol were used to calculate ΔH° values for the association reactions. Using these as estimates of ΔG° values for these reactions, by ignoring entropy and solvation effects, allowed comparison to measured stability constants. The calculated ΔH° values for formation of 3,5-dichloropyridine, pyridine, ethanol, and water complexes of the simple $\text{Co}(\text{porphine})(\text{NO}_2)$ complex were as follows, in order (values approximated from measured K by ignoring entropy effects are in parentheses, except where indicated): Cl_2py , -46.0 kJ/mol (-39.1 kJ/mol); py, -56.3 kJ/mol (-45.9 kJ/mol); EtOH, -38.2 kJ/mol (measured values of $\Delta H^\circ = -28$ kJ/mol and $K = 9.8$ implies $\Delta G^\circ = -5.65$ kJ/mol and $\Delta S^\circ = -75$ J/K·mol); and MeOH, -41.2 kJ/mol (measurement not available due to decomposition).

The six-coordinate alcohol complexes $(\text{ROH})\text{CoTpivPP}(\text{NO}_2)$ in alcohol solutions fail to oxidize alkenes at room temperature, even though spectroscopic and structural evidence suggests that activation of the NO_2 ligand takes place to a significant degree. Our earlier measurement of the free energy for the oxo-loss half-reaction for the $\text{FeTpivPP}(\text{NO}_2)_2/\text{FeTpivPP}(\text{NO})$ ($+50$ kJ/mol) complex caused us to conclude that the transfer of an oxygen atom to triphenylphosphine from iron-bound NO_2 is driven thermodynamically by the large oxo-gain half-reaction for triphenylphosphine in formation of triphenylphosphine oxide.¹⁸ A value of $\Delta H^\circ = -309$ kJ/mol is reported for this gas phase oxo-gain half-reaction. The entropy term was ignored for this approximation. Oxidation of alkenes to epoxides and other oxygen-containing species proceeds exothermically, but with relatively small enthalpy changes. A representative group of oxo-gain half-reactions have ΔH° values in the range of -80 to -120 kJ/mol as shown in Table 4A. Clearly, for these standard oxo-transfer half-reactions from the (nitro)cobalt porphyrin complex to occur, the standard oxo-loss enthalpies of the porphyrin system cannot be more than $+80$ to $+120$ kJ, and ideally far less. The results of DFT calculations of standard heats of formation for representative $\text{LCoTPP}(\text{NO}_2)$ porphyrin complexes are listed in Table 4B. The resulting oxo-loss enthalpies are listed also. The standard oxo-loss enthalpy calculated for the five-coordinate species ($+103.5$ kJ/mol) is significantly smaller than any of the values for six-coordinate derivatives. The standard oxo-loss enthalpy values for the alcohol complexes ($+143.1$ and $+144.5$ kJ/mol for the EtOH and MeOH complexes, respectively) are very similar to those of the water complex ($+140.23$ kJ/mol) and nearly as large as that of the pyridine complex ($+154.42$ kJ/mol). This similarity suggests that even though there may be differences in activation of the nitro ligand toward oxo-transfer in different complexes, all these six-coordinate derivatives lack oxo-transfer reactivity because of the unfavorable thermochemistry.

As already mentioned, the observed trends in spectroscopic and structural data suggested that activation of the nitro ligand may vary with the coordination environment of the

(18) Frangione, M.; Frangione, M.; Port, J.; Baldiwal, M.; Judd, A.; Galley, J.; DaVega, M.; Linna, K.; Caron, L.; Anderson, E.; Goodwin, J. *Inorg. Chem.* **1997**, *36*, 1904–1911.

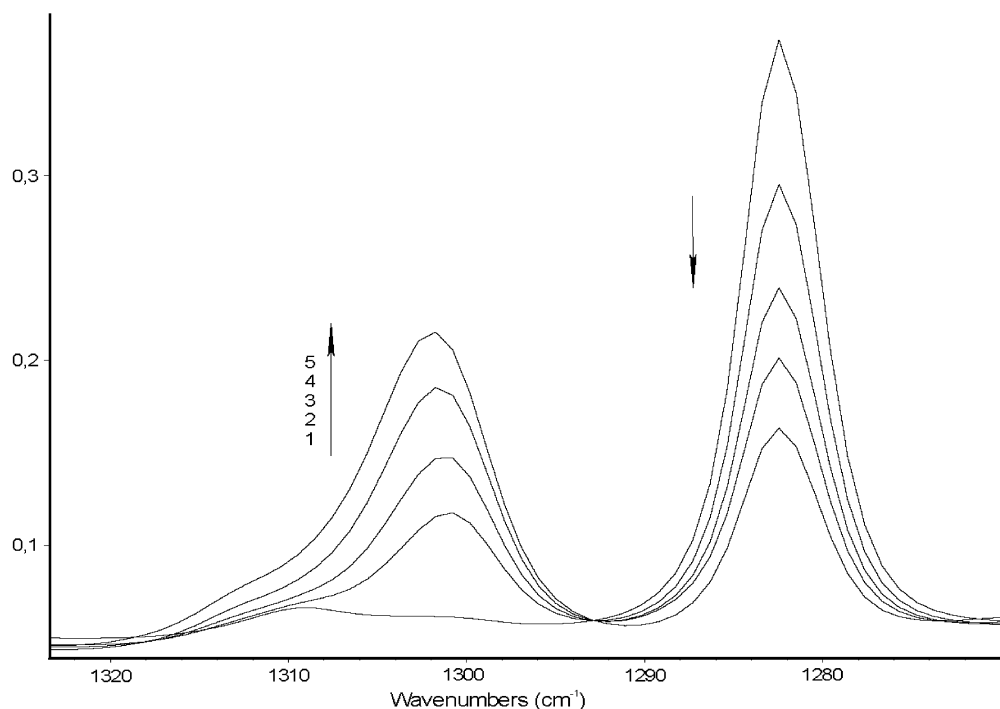


Figure 8. FTIR spectral changes observed in the $\nu_s(\text{NO}_2)$ range for a 5.17×10^{-3} M carbon tetrachloride solution of $(\text{C}_2\text{H}_5\text{OH})\text{CoTPP}(\text{NO}_2)$ in the presence of various concentrations of ethanol: $c_1 = 5.17 \times 10^{-3}$ M; $c_2 = 4.9 \times 10^{-2}$ M; $c_3 = 9.8 \times 10^{-2}$ M; $c_4 = 1.7 \times 10^{-1}$ M; $c_5 = 2.5 \times 10^{-1}$ M.

Table 4. (A) Standard Oxo-Gain Enthalpies for Formation of Epoxides from Alkenes. (B) Standard Enthalpies of Oxo-Loss Predicted by DFT Calculations Using Co(porphine) Core. (C) Standard Enthalpies of Oxo-Transfer Calculated from Data in Sections A and B^a

Part A						
oxo-acceptor, X	oxo-gain enthalpy, kJ/mol	enthalpy of formation, X, kJ/mol ^b	enthalpy of formation, XO, kJ/mol			
cyclohexene	-117	-4	-121			
allyl bromide	-88	48	-40			
propylene	-119	21	-98			
ethylene	-105	52	-53			
triphenylphosphine ^c	-309					
Part B						
L ligand of oxo-donor complex LCoP(NO ₂)	oxo-loss enthalpy by DFT, kJ/mol	oxo-transfer activation energy with Me ₃ P by PM3, kJ/mol				
none	+104	+255				
CH ₃ OH	+145	+251				
CH ₃ CH ₂ OH	+143	+251				
H ₂ O	+140	+243				
pyridine	+154	+201				
Part C						
	predicted oxo-transfer reaction energies, kJ/mol					
	cyclohexene	allyl bromide	propylene	ethylene	triphenylphosphine	
none	+104	-13	16	-15	-1	-205
CH ₃ OH	+145	28	57	26	40	-164
CH ₃ CH ₂ OH	+143	26	55	24	38	-162
H ₂ O	+140	23	52	21	35	-159
pyridine	+154	37	66	35	49	-155

^a All values are at 298.15 K. ^b Reference 19. ^c Reference 20.

cobalt center. Applying semiempirical methods to transition state energies combines the assessment of oxo-loss from the perspectives of ligand activation and oxo-transfer enthalpies. For this analysis a model system involving a (nitro)cobalt

porphine complex undergoing bimolecular oxo-transfer to trimethylphosphine was explored. These results are listed in Table 4B. While the reliability of the semiempirical calculations is limited for energy calculations, the values are rather close. Our attempts to improve these calculations with DFT models were not successful.

A similar semiempirical analysis of the thermochemistry has been undertaken for the peroxyxynitro intermediate of the catalytic cycle proposed earlier. In this approach the proposed peroxyxynitro intermediate is formed from reaction of molecular oxygen with the air-sensitive nitrosyl cobalt(II) porphyrin. The driving force for oxo-loss from this nitrogen-bound peroxyxynitrite ligand is predicted to be significantly more exothermic. Our semiempirical PM3 calculations yield standard oxo-loss enthalpies for five-coordinate CoP(NO₂O) as -270 kJ/mol and for (py)CoP(NO₂O) as -151 kJ/mol. In this case intermediate dioxygen activation is predicted to be very strong, but catalysis limited by the thermochemistry of the second oxo-transfer step. While there is no direct evidence that it is a pathway in this system, the loss of an oxygen atom from peroxyxynitrite to oxidize dioxygen to form ozone is thermochemically possible with the five-coordinate system, as was suggested by Castro for (nitro)iron complexes.³ The oxo-gain enthalpy of oxygen is +142 kJ/mol.¹⁹ It is clear, however, that with such large predicted differences in oxo-loss enthalpies for the peroxyxynitro and nitro complexes, the mechanisms and products of these distinct oxo-transfer steps are likely to be different and would account for the loss of specificity in the observed catalytic oxidation reaction.

(19) NIST Thermochemical Data. <http://webbook.nist.gov/chemistry/name-ser.html>.

(20) Holm, R. H. *Chem. Rev.* **1987**, *87*, 1401-1449.

Conclusions

Oxygenated products of catalytic oxidation, specifically alcohols that may be prepared from alkenes, can function as ligands for (nitro)cobalt(III) porphyrins. Their presence at low concentration allows oxidation catalysis to continue in solution due to their weak coordination that allows the reactive pentacoordinate nitro complex to remain in equilibrium. Although the nitro ligand in these water and methanol complexes appears to have a structure more similar to that in the five-coordinate (nitro)cobalt porphyrin system than to that in the corresponding pyridine complex, its reactivity is governed by the overall thermodynamics of the oxygen-transfer reaction.

Acknowledgment. We gratefully acknowledge the U.S. Civilian Research and Development Foundation (CRDF, 12001) and the National Foundation for Science and

Advanced Technologies (NFSAT, CH 053-02) for financial support of this work. This research was also funded in part by the Horry County Higher Education commission's support of Coastal Carolina University's Academic Enhancement Grants Program. Michael Zaworotko at USF assisted with the X-ray diffraction studies and NSF-DMR for the use of the X-ray machine.

Supporting Information Available: Figure S1: Temperature-dependent FTIR spectral changes in the range of $\nu_s(\text{NO}_2)$ observed for carbontetrachloride solution of 1.1×10^{-2} M $(\text{C}_2\text{H}_5\text{OH})\text{CoTPP}(\text{NO}_2)$ and 5.14×10^{-1} M ethanol (1, 18 °C; 2, 25 °C; 3, 35 °C; 4, 45 °C; 5, 55 °C; 6, 65 °C). Table S1: Bond lengths [Å] and angles [deg] for $(\text{H}_2\text{O})\text{CoTpivPP}(\text{NO}_2)$. Table S2: Bond lengths [Å] and angles [deg] for $(\text{CH}_3\text{OH})\text{CoTpivPP}(\text{NO}_2)$. This material is available free of charge via the Internet at <http://pubs.acs.org>.

IC048701A